Numerical Dosimetric Investigation of a WPT Charger

Report

Quotation #5210058-A to BURY GmbH & Co KG

Document Version 1.1 / 28th Jan, 2022

Authors: David Schäfer, Jan Buchholz, Winfried Simon

IMST GmbH
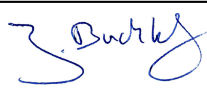Carl-Friedrich-Gauß-Str. 2–4
47475 Kamp-Lintfort
Germany

Information

File Name	Report_WCA-CS-NFC-LCI_V1.1.pdf
Initial Date	28th Sept, 2021
Page count	18

Versions

Release Date	Version	Author	Comments
28th Sept, 2021	1.0	David Schäfer	Initial version
28th Jan, 2022	1.1	David Schäfer	Typos and Limits table corrected

Approval

Name	Job Title	Date	Signature
David Schäfer	Project leader, simulations	28th Jan, 2022	
Jan Buchholz	Simulations	28th Jan, 2022	
Winfried Simon	Team leader "EM Modeling"	28th Jan, 2022	

Device Under Test (DUT)

Type of DUT	Wireless Power Transfer Charger
Model Name	WCA CS NFC LCI
FCC ID	QZ9-WCACS
ISED Certification No.	5927A-WCACS
Frequency band	111 kHz
Antennas / Coils / Active elements	Three coils
Applicant	BURY GmbH & Co KG Robert-Koch-Str. 1-7 32584 Löhne, Germany Contact: Johann Dshus

Human Exposure Limits

Specific Absorption Rate (47 CFR Ch. I § 1.1310 10-1-20 Edition)

Condition	Uncontrolled Environment (General Public)		Controlled Environment (Occupational)	
	SAR Limit	Mass Avg.	SAR Limit	Mass Avg.
SAR averaged over the whole body mass	0.08 W/kg	whole body	0.4 W/kg	whole body
Peak spatially-averaged SAR	1.6 W/kg	1 g of tissue*	8 W/kg	1 g of tissue*
Peak spatially-averaged SAR for extremities, such as hands, wrists, feet, ankles, and pinnae	4.0 W/kg	10 g of tissue*	20 W/kg	10 g of tissue*
* Defined as a tissue volume in the shape of a cube				

Evaluation Results

Quantity inside flat phantom	Result*	Below exposure limit set by ...				
		ICNIRP 2020	47 CFR § 1.1310	RSS-102 Issue 5	1999/ 519/EC	RPS S-1
$SAR_{1g, max}$	46.057 mW/kg	—**	Yes	Yes	—	—
$SAR_{10g, max}$	21.376 mW/kg	Yes	Yes	Yes	Yes	Yes
** Not applicable combinations were indicated as "—"						

Contents

List of Figures

List of Tables

1   Introduction

1.1   Objective

The objective is the numerical dosimetric investigation of one Wireless Power Transfer (WPT) Charger (further referred to as "device under test" or "DUT") designed by BURY GmbH & Co KG (further referred to as "applicant"). In particular the Specific Absorption Rate (SAR, heat damage hazard) was investigated and compared to exposure limits specified by ICNIRP [1], FCC [2], ISED [3], EUCO [4] and the ARPANSA [5].

1.2   Simulation Method

All simulations were done with the Finite Difference Time Domain (FDTD) simulation tool Empire XPU [6]. A numerical model of the DUT was generated and validated by measurements of the magnetic field in its vicinity and measured inductance of the charging coil. The spatially averaged SAR inside a flat phantom (human body part model) was investigated.

1.3   DUT Description

The 5 W, triple coil, wireless power charger "WCA CS NFC LCI" (further referred to as "device under test" or "DUT") can be used to charge portable devices like smart-phones (further referred to as "WPT receiver"). It is designed to be integrated into a vehicle, e.g. into the center console of a car. The DUT operates at a frequency of 111 kHz and features three charging coils. During operation only one of the three coils is excited/charging at a time. Which coil is used for charging is chosen by the DUT itself, depending on the placement of the WPT receiver device. A photo of the DUT is depicted in Figure 1.


Figure 1: Photo of the DUT

1.4   Setup for Reference Measurement

A validation of the numerical model was carried out by comparing the simulated magnetic field in the vicinity of the DUT with a reference measurement. The measurement was done on the behalf of the applicant by the lab of "CTC advanced GmbH" with the setup depicted in Figure 2. They used a "DASY8" positioner system from Speag and a "MAGPy-H3D" magnetic field probe with a $1\,\text{cm}^2$ "sensor size (loop)" and $6.6\,\text{mm}$ "sensor center to tip distance". The measurements were done for a series production equivalent device, running in a testing operating mode at a fixed coil current of $3.0\,\text{A}$ RMS. The applicant pre-determined this to be the maximum expectable coil current during charging a WPT receiver. No WPT receiver was present during the reference measurements of the magnetic field.

Preliminary investigation showed that the worst-case configuration is given when the center coil is excited, so only this operation state was considered. For the actual reference measurement the field probe was located directly above the xy-center of the center coil. A line measurement of the magnetic field strength was performed by lifting the probe upwards along the coil axis to different z-distances from the DUT. Figure 2 (a) show the lowest possible position of the field probe (touch position).

(a)   (b)
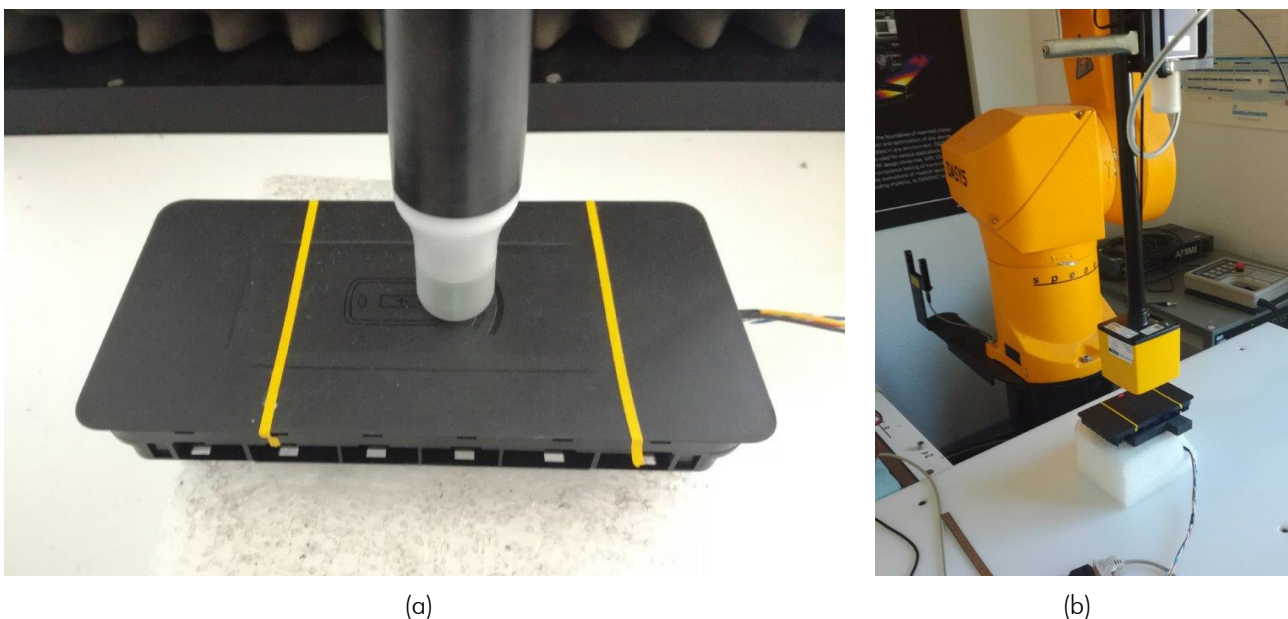
Figure 2: Measurement setup from the external lab of "CTC advanced GmbH", showing (a) a close-up of the "MAGPy-H3D" probe in touch position and (b) the "DASY8" positioner (with a different probe installed than used for the measurements).

2 EM Simulation Model

2.1 Model Setup

The simulation model of the DUT is based on STEP CAD data provided by the applicant. The data was imported into Empire XPU, whereby the coordinate origin of the STEP files was maintained. Figure 3 shows a top and bottom 3D view of the simulation model.

(a)   (b)
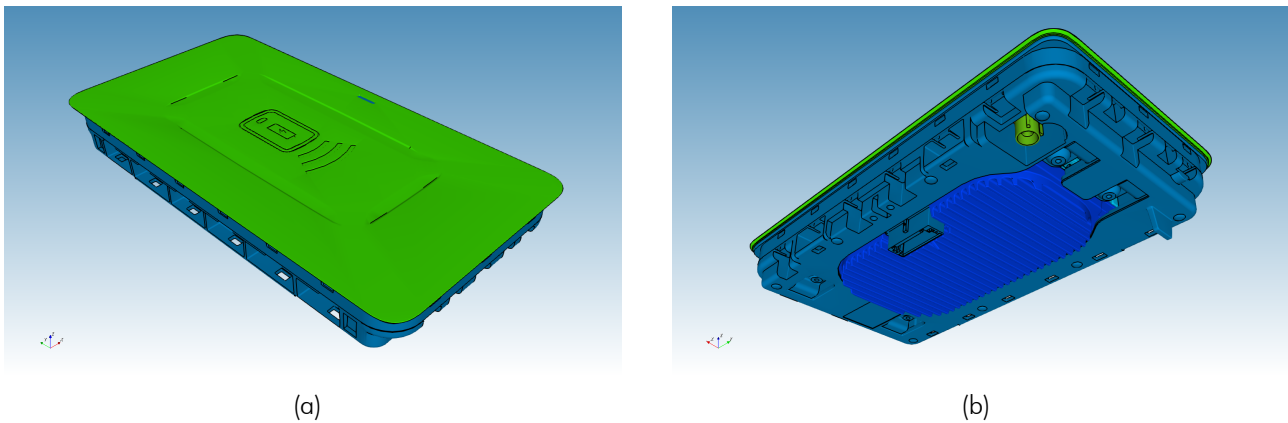
Figure 3: Geometry of the Empire simulation model of the DUT, showing the outer view on the top (a) and bottom (b) side.

In Figure 4 the internal components are visible, including the three WPT charging coils (in green). The charging coil (central coil) can be seen in the middle, being overlapped by the sideways coils. Its middle point is located at $x = y = 0\,\text{mm}$, $z = -3.51\,\text{mm}$ and the top side of the DUT housing is at $z = 0.0\,\text{mm}$.
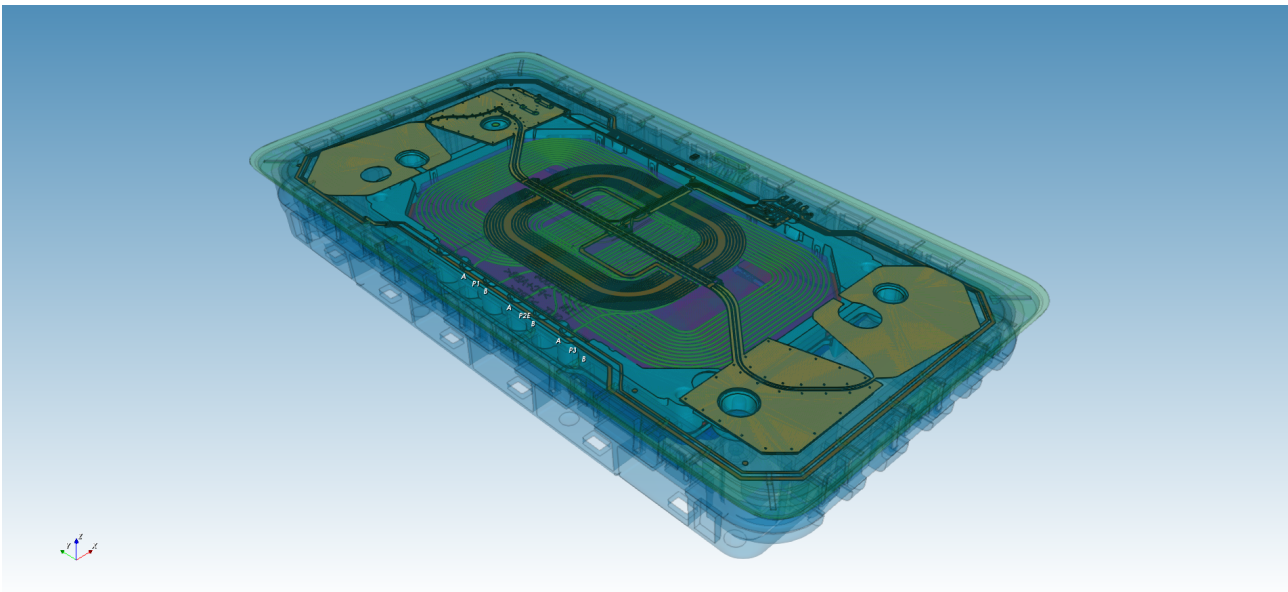
Figure 4: Geometry of the Empire simulation model of the DUT. The housing of the DUT is set transparent to show the internal components.

Figure 5 shows an exploded view of the most important components of the simulation model. Based on the applicants information the material properties were set as follows:

(a) Top PCB (Copper traces, $\sigma = 58 \cdot 10^6$ S/m)

(b) WPT coils (Copper, $\sigma = 58 \cdot 10^6$ S/m)

(c) Ferrite plate ($\mu_r = 850$, $tan(\delta) = 0.0153$)

(d) Bottom PCB shielding (Steel-Stainless JIS SUS430, $\sigma = 1.66 \cdot 10^6$ S/m)

(e) Bottom PCB components (PEC, $\sigma = Inf$)

(f) Bottom PCB (Copper traces, $\sigma = 58 \cdot 10^6$ S/m)

(g) Heat sink ($AlSi_{12}Cu_1Fe$, $\sigma = 17.4 \cdot 10^6$ S/m)
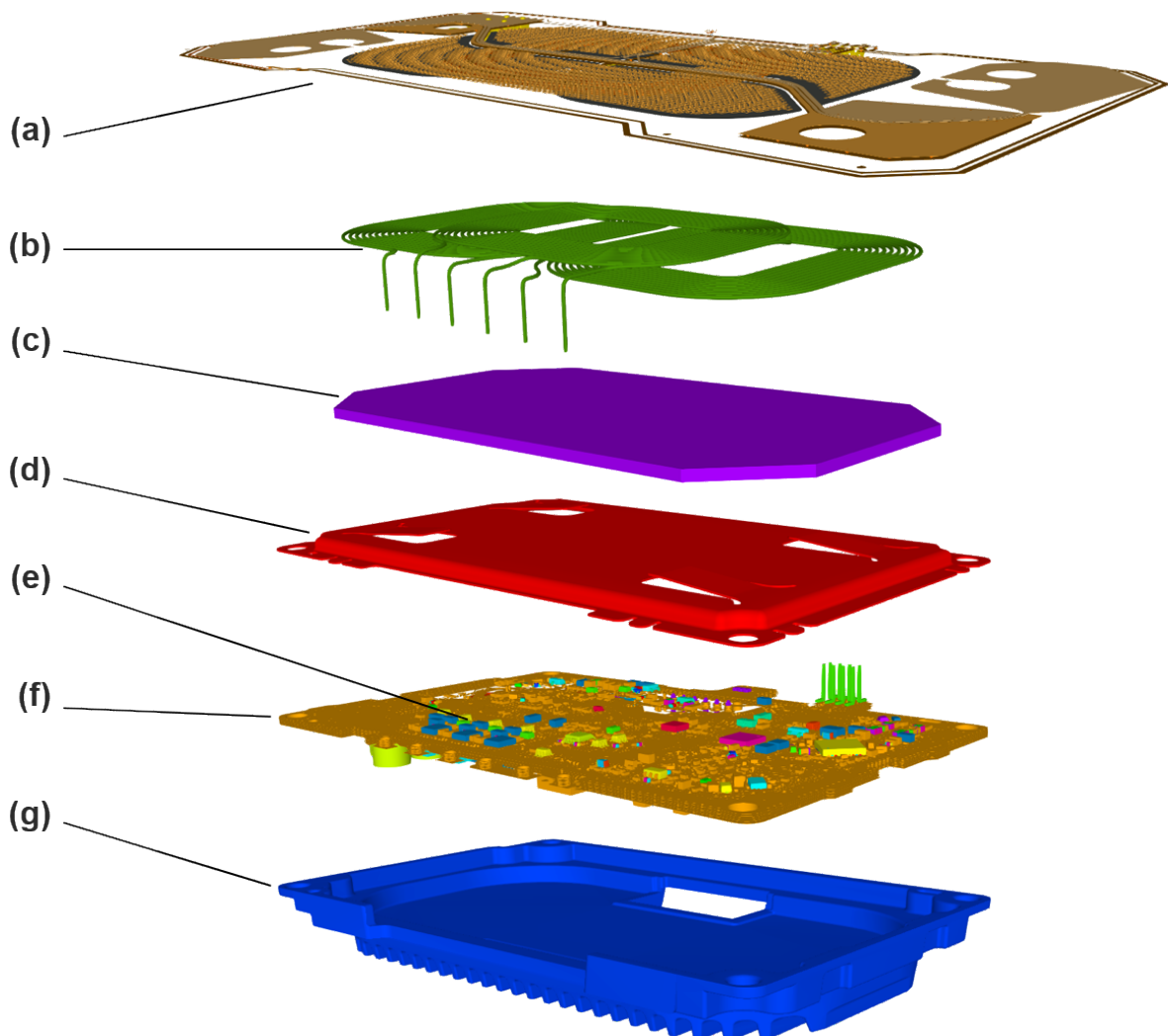
Figure 5: Geometry of the Empire simulation model of the DUT, showing an exploded view of the top PCB (a), the WPT coils (b), ferrite (c), bottom PCB shielding (d), bottom PCB components (e), bottom PCB (f) and the heat sink (g).

From the top PCB a grid of small rings and the graphite coating were removed from the simulation model, because they only have a small affect on the assessed quantities but require an excessively fine mesh.

2.2 Model Check

The simulation model was checked by comparing the simulated magnetic fields with the reference measurement (cf. section 1.4). During measurement the central coil was excited with the maximum expectable current of $3.0\,\text{A}$ (RMS) at a frequency of $111\,\text{kHz}$. The two sideways coils were inactive, so during the simulation their inputs were terminated with non-excited ports with $1\,\text{k}\Omega$ impedance. The simulation setup was unperturbed, meaning that it didn't include a WPT receiver device or phantom (human body model).

2.2.1 Magnetic Fields

Figure 6 shows a yz-cutplane for the simulated magnetic field strength through the center of the DUT. It can be seen how the main PCBs ground and the ferrite confine the main part of the magnetic field to the dedicated WPT receiver location above the DUT.
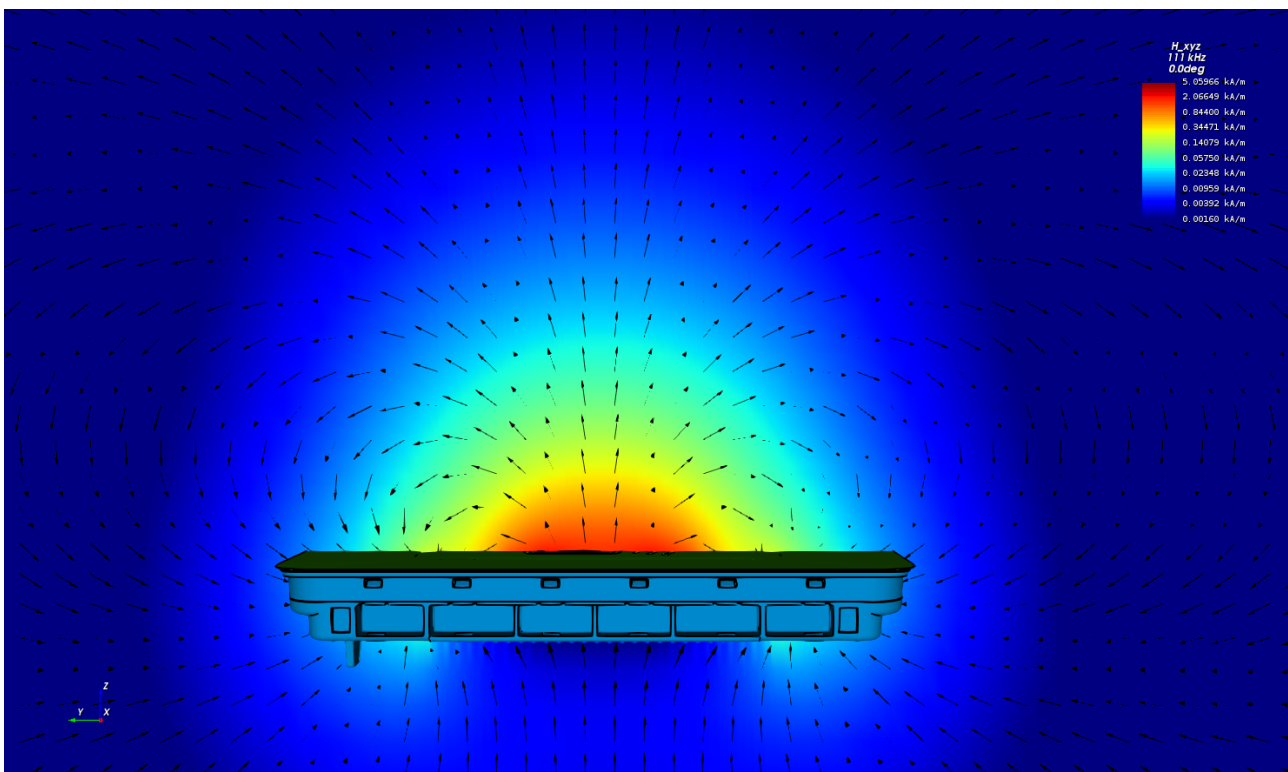
Figure 6: The simulated magnetic field displayed on a yz-plane through the DUT.

Analogue to the setup of the measurement (cf. section 1.4) the simulated magnetic field (H-field) strength was evaluated along the axis of the central coil. The measurements start at $z = 7\,\text{mm}$, which approximately corresponds to the "sensor center to tip distance" of the "MAGPy-H3D" field probe. The simulated line starts at the top of the DUTs housing at ($z = 0\,\text{mm}$). As Figure 7 depicts, the simulated H-field is in very good agreement with the measurement.
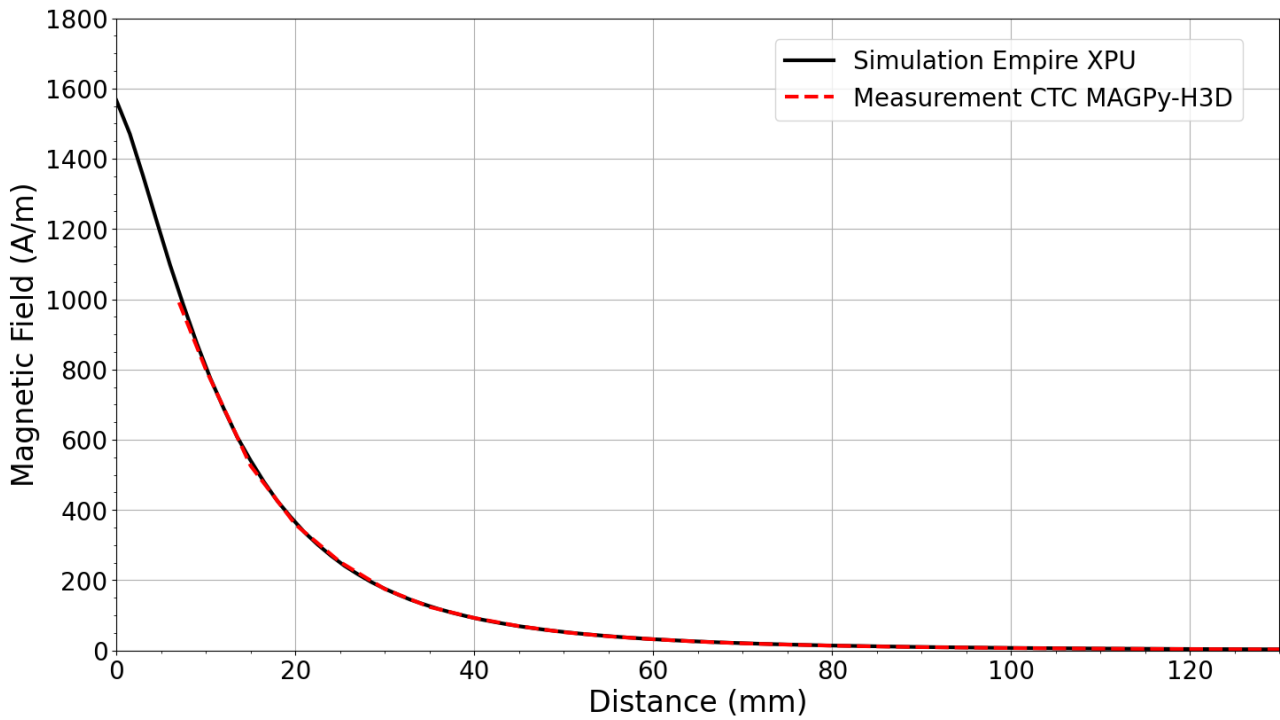
Figure 7: Curves for the line evaluation of the H-field (RMS values). The top of the DUT dielectric housing is located at $z = 0.0\,\text{mm}$.

2.2.2   Coil Inductance

In addition to the magnetic fields also the inductance of the coil was used to check the simulation model. With a relative deviation of $+5.88\,\%$ (cf. Table 1) the simulated inductance is in good agreement with the measurement.

|	Measured	Empire	Deviation
Coil Inductance	$11.338\,\mu\text{H}$	$12.005\,\mu\text{H}$	$+5.88\,\%$

Table 1: Measured and simulated inductance.

2.2.3   Conclusion of Model Validation

It can be concluded, that simulated magnetic field strength and inductance are in good agreement (cf. Figure 7 and Table 1) with the measurements from the applicant and the external lab of "CTC advanced GmbH", indicating the accurate setup of the Empire simulation model.

3   SAR Evaluation

For the evaluation of the Specific Absorption Rate (SAR) a box shaped flat phantom was added to the simulation model. The setup resembles the situation of someone touching the DUT just after a receiver removal which was in "charging mode" at maximum field. For the SAR evaluation the coil current could have been reduced according to the search mode duty cycle, but the continuous maximum expectable coil current was retained throughout the investigation.

<table>
<tr><td>(a)</td><td>(b)</td></tr>
</table>
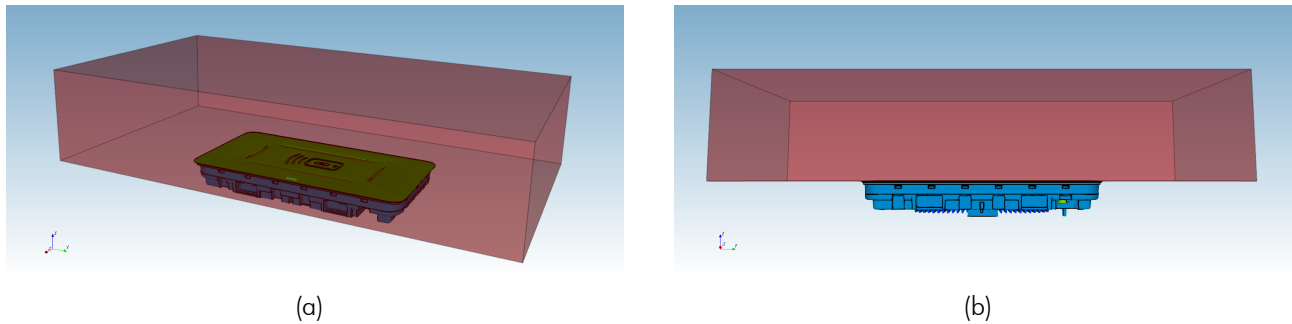
Figure 8: Geometry of the flat phantom in 3D view (a) and side view (b) showing it is in touch with the DUTs housing.

The phantom was centred (xy-direction) above the active coil at closest possible $z-$distance, virtually touching the top side of the DUT dielectric housing as shown in Figure 8. With respect to the CAD coordinate system origin, the phantoms bottom side (side towards DUT) is located at $z = 0.0\,\text{mm}$. The dimensions and the material properties of the phantom are as follows:

1. Geometric Size: $d_x \cdot d_y \cdot d_z = 180\,\text{mm} \cdot 340\,\text{mm} \cdot 70\,\text{mm}$
2. Relative Permittivity: $\epsilon_r = 55$
3. Electrical Conductivity: $\sigma = 0.75\,\text{S/m}$
4. Mass Density: $\rho = 1000\,\text{kg/m}^3 = 1\,\text{g/cm}^3$

More details about the numerical model, like e.g. domain size, time step or total number of mesh cells, can be found in the appendix in section 4.1.

3.1   Simulation Results

Figure 9 shows the simulated 1g- and 10g-averaged SAR. Table 2 lists the corresponding maximum values and their positions.

Quantity	Maximum Value	Position of Maximum		
		x	y	z
SAR$_{1g,\,max}$	46.057 mW/kg	0.296 mm	-20.787 mm	0.25 mm
SAR$_{10g,\,max}$	21.376 mW/kg	0.205 mm	-20.787 mm	0.25 mm

Table 2: SAR maximum values with their corresponding positions.
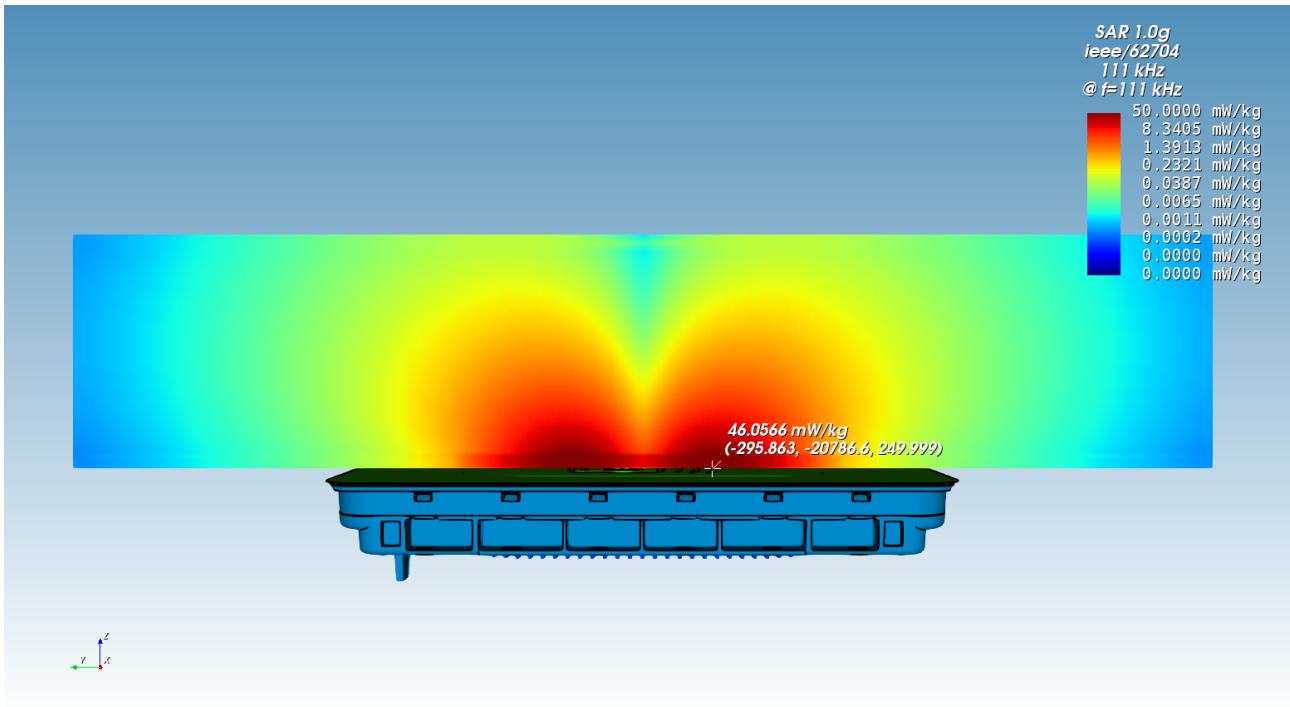
(a) Simulated 1g-averaged SAR
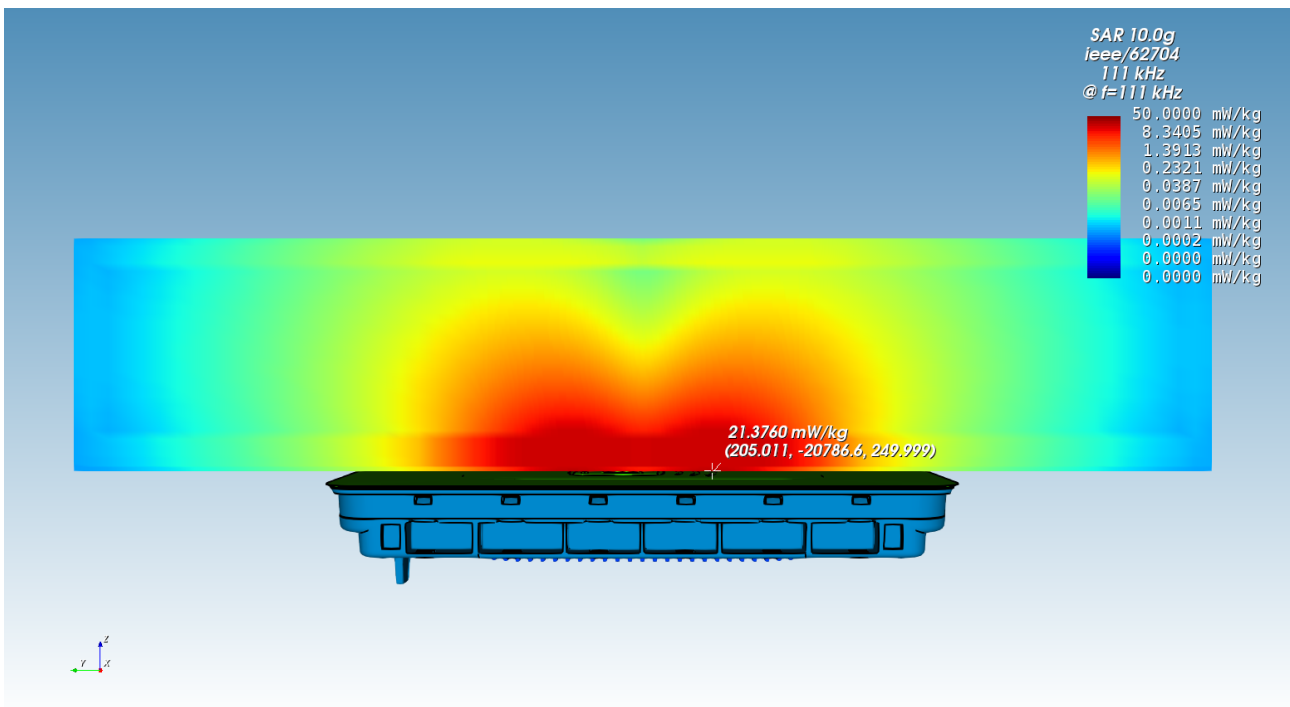
(b) Simulated 10g-averaged SAR

Figure 9: Cutplanes through the maxima of the simulated 1g-averaged SAR (a) and 10g-averaged SAR (b) inside the flat phantom. The phantom geometry is not visible. The discontinuities at the phantom boundaries are caused by the averaging algorithm (cf. [7, Section 6.2.2]).

3.2   Tolerance Analysis

To analyse the accuracy of the results for the numerical model presented in section 3.1 (further referred to as "reported model"), several variants were created and simulated. Table 3, 4, 5 and 6 show the maximum SAR for the investigated variants as well as their relative deviation from the reported model.

Phantom z-Position	0.00 mm	0.5 mm
$SAR_{1g, max}$	46.057 mW/kg	42.038 mW/kg
$SAR_{10g, max}$	21.376 mW/kg	19.689 mW/kg
$SAR_{1g, max}$-Deviation	0 %	−8.73 %
$SAR_{10g, max}$-Deviation	0 %	−7.89 %

Table 3: SAR results for different phantom positions. The first data column corresponds to the reported model (cf. section 3.1).

Mesh Resolution	3.8 MCells	8.1 MCells
$SAR_{1g, max}$	46.057 mW/kg	46.287 mW/kg
$SAR_{10g, max}$	21.376 mW/kg	21.385 mW/kg
$SAR_{1g, max}$-Deviation	0 %	+0.50 %
$SAR_{10g, max}$-Deviation	0 %	+0.04 %

Table 4: SAR results for different mesh resolutions. The first data column corresponds to the reported model (cf. section 3.1).

Domain Size	$380 \cdot 540 \cdot 383.75$ mm	$570 \cdot 810 \cdot 575.625$ mm
$SAR_{1g, max}$	46.057 mW/kg	46.085 mW/kg
$SAR_{10g, max}$	21.376 mW/kg	21.386 mW/kg
$SAR_{1g, max}$-Deviation	0 %	+0.06 %
$SAR_{10g, max}$-Deviation	0 %	+0.05 %

Table 5: SAR results for different simulation domain sizes. The first data column corresponds to the reported model (cf. section 3.1). The simulation domain was enlarged symmetrically in all spatial directions.

Time/Convergence	20 Msteps	40 Msteps
Energy Decay	105.29 dB	106.35 dB
$SAR_{1g, max}$	46.057 mW/kg	46.059 mW/kg
$SAR_{10g, max}$	21.376 mW/kg	21.378 mW/kg
$SAR_{1g, max}$-Deviation	0 %	+0.004 %
$SAR_{10g, max}$-Deviation	0 %	+0.009 %

Table 6: SAR results for different number of total time steps. The first data column corresponds to the reported model (cf. section 3.1).

3.3   Conclusion of SAR Evaluation

Summarizing the numerical dosimetric investigation of the DUT, the following can be stated:

1. The simulated magnetic field strength is in good agreement with the measurements (cf. section 2.2), indicating the accurate setup of the DUT simulation model (without phantom).

2. The investigated scenario follows the worst-case assumption that:

    (a) The flat phantom is in direct contact with the DUT.

    (b) The DUT is exciting its center coil with the maximum expectable current, despite the fact that no receiver device is present.

    (c) The search mode duty cycle is neglected.

3. The determined maximum 1g-averaged SAR is $46.057\,\mathrm{mW/kg}$.

4. The determined maximum 10g-averaged SAR is $21.376\,\mathrm{mW/kg}$.

5. With respect to the statements above, the conclusion of this numerical dosimetric investigation report is, that the DUT does not exceed the exposure limits for SAR specified by ICNIRP [1], FCC [2], ISED [3], EUCO [4] and ARPANSA [5]. A tabular evaluation can be found at the beginning of the report.

4   Appendix

4.1   Specific Information for SAR Computational Modelling

Computational resources Computation was performed on an AMD Ryzen 9 5950X 16-core processor with $4.899\,\text{GB}$ memory usage.

FDTD algorithm implementation and validation cf. [8]

Computing peak SAR from field components cf. [8]

1g-averaged SAR procedures cf. [7, 8]

Computational parameters for reported model:

> **Cell Size (min/max):** $0.4128\,\text{mm}$ / $10.57\,\text{mm}$
>
> **Domain Size:** $380 \cdot 540 \cdot 383.75\,\text{mm}$
>
> **Total amount of mesh cells:** approx. 3.8 million
>
> **Time step:** $3.52528 \cdot 10^{-13}\,\text{s}$
>
> **Total number of time steps:** approx. 20 million
>
> **Simulation time:** approx. 3 hours and 51 minutes
>
> **Simulation speed:** 10741 million cells per second ($10.741\,\text{GCells/s}$).
>
> **Excitation method:** Gaussian pulse with $f_0 = 0\,\text{Hz}$, $f_{\text{BW}} = 50\,\text{MHz}$

Phantom model implementation cf. section 3

Tissue dielectric parameters cf. section 3

Transmitter model implementation and validation cf. section 2

Test device positioning cf. section 3

Steady state termination procedures A Gaussian pulse was used for the excitation and the simulation was terminated when the energy has dissipated to more than $105\,\text{dB}$.

Test results cf. section 3

4.2   Abbreviations

Abbreviation	Description
CAD	Computer Aided Design
DUT	Device Under Test
EIAV	Averaged Internal Electric Field
EM	Electro Magnetic
FDTD	Finite Difference Time Domain
PCB	Printed Circuit Board
RF	Radio Frequency
RMS	Root Mean Square
SAR	Specific Absorption Rate
S/m	Siemens per meter $= 1/(\Omega m)$

Table 7: Abbreviations.

5 References

[1] International Commission on Non-Ionizing Radiation Protection (ICNIRP), "ICNIRP Guidelines for limitting Exposure to Electromagnetic Fields (100 KHz to 300 GHz)," 2020.

[2] Federal Communications Commission (FCC, USA), "FCC Limits for Specific Absorption Rate (SAR), 47 C.F.R. § 2.1093," 2012.

[3] Innovation, Science and Economic Development Canada (ISED, Canada), "RSS-102 Issue 5 - Radio Frequency (RF) Exposure Compliance of Radiocommunication Apparatus (All Frequency Bands)," March 2015.

[4] European Council, "Council Recommendation of 12 July 1999 on the limitation of exposure of the general public to electromagnetic fields (0 Hz to 300 GHz), 1999/519/EC," July 1999.

[5] Australian Radiation Protection and Nuclear Safety Agency (ARPANSA), "Standard for Limiting Exposure to Radiofrequency Fields – 100 kHz to 300 GHz - Radiation Protection Series S-1, RPS S-1," February 2021.

[6] IMST GmbH. (2020, August) Empire XPU. Carl-Friedrich-Gauß-Str. 2-4, 47475 Kamp-Lintfort, Germany. [Online]. Available: http://empire.de

[7] "IEC/IEEE International Standard – Determining the peak spatial-average specific absorption rate (SAR) in the human body from wireless communications devices, 30 MHz to 6 GHz - Part 1: General requirements for using the finite-difference time-domain (FDTD) method for SAR calculations," *IEC/IEEE 62704-1:2017*, pp. 1–86, 2017.

[8] IMST GmbH, "EMPIRE XPU - Code Verification according to IEC/IEEE P62704-1."